NASA Technical Memorandum 101692

Real-Time Flight Test Analysis and Display Techniques for the X-29A Aircraft

John W. Hicks and Kevin L. Petersen

November 1988

NASA
National Aeronautics and
Space Administration

NASA Technical Memorandum 101692

Real-Time Flight Test Analysis and Display Techniques for the X-29A Aircraft

John W. Hicks and Kevin L. Petersen
Ames Research Center, Dryden Flight Research Facility, Edwards, California

1988

NASA
National Aeronautics and
Space Administration
Ames Research Center
Dryden Flight Research Facility
Edwards, California 93523-5000

REAL-TIME FLIGHT TEST ANALYSIS AND DISPLAY TECHNIQUES FOR THE X-29A AIRCRAFT

John W. Hicks
Aerospace engineer
and
Kevin L. Petersen
Chief, Vehicle Technology Branch
NASA Ames Research Center
Dryden Flight Research Facility
P.O. Box 273
Edwards, California 93523-5000
U.S.A.

SUMMARY

The X-29A advanced technology demonstrator flight envelope expansion program and the subsequent flight research phase gave impetus to the development of several innovative real-time analysis and display techniques. These new techniques produced significant improvements in flight test productivity, flight research capabilities, and flight safety.

These techniques include real-time measurement and display of in-flight structural loads, dynamic structural mode frequency and damping, flight control system dynamic stability and control response, aeroperformance drag polars, and aircraft specific excess power. Several of these analysis techniques also provided for direct comparisons of flight-measured results with analytical predictions. The aeroperformance technique was made possible by the concurrent development of a new simplified in-flight net thrust computation method. To achieve these levels of on-line flight test analysis, integration of ground and airborne systems was required. The capability of NASA Ames Research Center, Dryden Flight Research Facility's Western Aeronautical Test Range was a key factor to enable implementation of these methods.

NOMENCLATURE

AR	analog reversion (flight control system mode)
BFF	body-freedom flutter
c.g.	center of gravity
C	loads calibration coefficient
C_D	coefficient of drag
C_L	coefficient of lift
D	aircraft drag, lb
DR	digital reversion (flight control system mode)
FCS	flight control system
F_{ex}	excess thrust, lb
F_g	gross thrust, lb
F_{np}	net propulsive force, lb
FM	frequency modulation
HPC	high-pressure compressor
L	aircraft lift, lb
LPT	low-pressure turbine
n_x	aircraft longitudinal acceleration, g
n_y	aircraft lateral acceleration, g
n_z	aircraft normal acceleration, g
ND	normal digital (flight control system mode)
p	roll rate, deg/sec
PCM	pulse-code modulation
P_s	specific excess power, ft/sec
p_{s_0}	freestream static pressure, lb/in.^{2}

p_{s6}	afterburner inlet static pressure, lb/in.^{2}
p_{s7}	exhaust nozzle inlet static pressure, lb/in.^{2}
PSL	Propulsion System Laboratory (NASA Lewis)
pT_{58}	turbine discharge total pressure, lb/in.^{2}
q	pitch rate, deg/sec
$\bar{q}$	dynamic pressure, lb/ft^2
r	yaw rate, deg/sec
RIG	real-time interactive graphics system
S	reference wing area, ft^2
SGTM	simplified gross thrust method
SNTM	simplified net thrust method
V_t	true airspeed, ft/sec
WATR	Western Aeronautical Test Range
W_t	aircraft gross weight, lb
α	angle of attack, deg
β	angle of sideslip, deg
δ_a	differential flaperon deflection, deg
δ_c	canard deflection, deg
δ_f	symmetric flaperon deflection, deg
δ_{ps}	pitch stick deflection, in.
δ_r	rudder deflection, deg
δ_s	strake flap deflection, deg
δ_{ys}	lateral stick deflection, in.
ϕ	bank angle, deg
μ	loads strain gage measurement
θ	pitch attitude, deg

1. INTRODUCTION

Beginning with the X-29A maiden flight in December of 1984, a key program objective has been to evaluate several integrated advanced technologies for future military applications. The X-29A advanced technology demonstrator flight envelope expansion program and the subsequent flight research phase gave impetus to the development of several innovative real-time analysis and display techniques. Most of these developments resulted from the nature of the unique technologies to be evaluated and critical requirements for safety-of-flight assurance. The forward-swept wing design and the concern of its inherent tendency toward structural wing divergence created the need for constant in-flight structural loads monitoring. It was especially important to monitor the interaction between the vehicle bending and torsion loads against load limit envelopes for critical airframe members. In order to monitor critical structural modes, the dynamic characteristics of the structure were determined from real-time computation of the frequency and damping of five critical structural modes that were in turn graphically compared against predictions during the mission.

The large subsonic airframe negative static margin of 35 percent required high levels of augmentation to artificially stabilize the aircraft. The performance of the flight control system thus became a key factor in the flight envelope expansion. It was desirable to calculate and monitor system stability margins derived from open-loop frequency response characteristics in real time. In addition to monitoring stability in the frequency domain, actual aircraft time responses were compared with predicted responses from linear aircraft simulation models during flight. Although not safety-of-flight critical, real-time aeroperformance analysis in terms of in-flight net thrust and aircraft lift and drag polars would allow for immediate evaluation of aircraft maneuver technique and data quality to insure premium postflight data results and minimum flight repeats.

Such sophisticated real-time analyisis and display required careful integration of the aircraft telemetry data downlink system and the NASA Western Aeronautical Test Range (WATR) mission control facility.

This paper describes the primary features and analytical methods of each technique. It also summarizes how the techniques were used during flight to enhance flight safety and increase flight productivity. A description of the WATR facility is given along with a discussion of the flight data processing flow. Examples of data processed and the flight data displays are shown.

2. X-29A AIRCRAFT DESCRIPTION

The X-29A is an advanced technology demonstrator developed by the Grumman Aerospace Corporation (Bethpage, New York) in partnership with the Defense Advanced Research Projects Agency, NASA, and the Air Force. This small, single-seat fighter-type aircraft's (fig. 1) technologies include the 30° forward-swept wing that includes a thin, supercritical airfoil section with graphite-epoxy upper and lower wing skins configured to inhibit wing structural divergence. Other technologies are the close-coupled canard-wing configuration, a three-surface pitch control system, an automatic wing camber control mode, a large negative static margin, and a triplex digital fly-by-wire flight control system.

The aircraft is powered by a single General Electric (Lynn, Massachusetts) F404-GE-400 afterburning turbofan engine. The engine thrust rating is 16,000 lb of static thrust at sea level. Further details of the X-29A configuration and the technology benefits can be found in reference 1.

3. AIRCRAFT DATA ACQUISITION SYSTEM

All pulse-code modulation (PCM) data was encrypted and telemetered to the ground as a single uncalibrated serial PCM stream along with some high-response frequency modulation (FM) data. The instrumentation system schematic can be seen in figure 2. The 10-bit PCM system sampled data 25 to 400 samples/sec, depending on the data frequency content desired by the various engineering disciplines. Including the FM system, a total of 691 aircraft parameters were measured. The data parameter set included measurements for structural loads and dynamics, flight controls, aircraft subsystems, stability and control, propulsion, aeroperformance, aerodynamic buffet, wing deflections, and external pressure distributions.

A pitot-static noseboom system provided air data information and angles of attack and sideslip from boom-mounted vanes. A set of body-mounted accelerometers provided measurement of aircraft c.g. accelerations. The aircraft had an extensive array of control surface position sensors and flight control system (FCS) performance parameters. The airframe was also heavily instrumented with strain gages and high-response structural dynamic accelerometers.

The thrust-calibrated engine was fully instrumented for real-time thrust calculation as well as postflight analysis using the traditional gas generator thrust calculation method. The unique real-time thrust measurement instrumentation consisted simply of eight static pressure measurements in the afterburner section along with a 20-probe measurement rake of the turbine exhaust total pressure. A schematic of just the real-time engine measurements is shown in figure 3.

4. TEST RANGE AND REAL-TIME SYSTEM

The NASA Ames Research Center, Dryden Flight Research Facility's Western Aeronautical Test Range, or WATR, is a large, highly integrated facility that provides aircraft and telemetry tracking; communications systems; a real-time data acquisition, processing, and display system; and a mission control center.

Current capabilities of the WATR include reception of up to two simultaneous downlink data streams from each research aircraft at a maximum rate of 1 Mbit/sec/stream. The data stream is decrypted, time tagged, compressed, converted to engineering units, limit checked, and stored in real time at a maximum rate of 200,000 words/sec/data stream. This storage area can hold 4096 calibrated parameters plus 3200 computed parameters for recording, further processing, or display.

There are three dedicated real-time minicomputers for on-line data processing and control of display apparatus. Two of these computers are Gould 32/6780 (Gould Electronics, Inc., Cleveland, Ohio) machines and one is a Gould 32/9780 system.

Data display capabilities in each of two identical mission control rooms include eighteen 8-channel strip charts, numerous cathode ray tube digital data displays of either the fixed update or continuous scroll type, color graphics displays, and conventional analog meters and discrete lights. A terminal, located in the mission control center, controls the selection of several different engineering color graphics displays

including aeroperformance, flight controls and stability and control, and structural dynamics and loads. A photograph of the mission control center is shown in figure 4. Details of the WATR configuration and operation can be found in references 2 and 3.

5. ANALYSIS AND DISPLAY TECHNIQUES

5.1 Structural Loads

The forward-swept wing's inherent tendency toward static structural divergence and the potential for high loads on the canard, wing flaperons, and strake flaps necessitated direct real-time monitoring of certain critical structural loads. The interaction and interrelationship between the component bending and torsional loads was of concern and required a cross plotting routine to display these loads relative to strength envelopes rather than displaying separate time histories (conventional stripcharts were also used). These data were plotted graphically and monitored continuously, particularly as the X-29A expanded its normal load factor envelope. Extensive loads analysis of these and other structural components was also conducted post-flight. Both symmetric and asymmetric loading were carefully explored through a series of flight clearance maneuvers (ref. 4). Point-to-point real-time loads clearance was critical for flight safety and productivity as the X-29A's flight and maneuver envelope was expanded.

Cross-plotting capabilities were used to display strength envelopes for various vehicle stations on the major aircraft components. These plots were generally in the form of bending/torsion interaction plots where structural limits are interdependent. Loads and flight parameters are computed on the Gould real-time computers and passed to the real-time interactive graphics (RIG) for display. Structural loads are computed from a conventional point load calibration where for shear, bending, or torque the general equation form is

$$\text{load} = C_1\mu_1 + C_2\mu_2 + \ldots + C_n\mu_n \qquad (1)$$

where μ represents the individual strain gage measurements and C represents ground load calibration coefficients derived from regression techniques.

Figure 5 shows the color graphics display with sample data from a windup turn maneuver where the wing and canard plots are of primary interest. The upper left plot of the display shows the left canard root loads; the upper right plot, the fuselage lateral and vertical bending loads; the lower left plot, the left wing root loads; and the lower right plot, the vertical tail root loads. On the canard, wing, and vertical tail plots, the horizontal axis is the torsional load, and the vertical axis is the bending load. During a maneuver, flight data are plotted with 80 and 100 percent design limit "boxes" or polygons superimposed with the general intent being to stay within the inner 80 percent box. Alternate pages are available that replace the lower right plot with a different wing load station. Digital parameters displayed to the left of the plots contain flight conditions and aircraft state parameters in the upper block. The lower block contains discrete load channel outputs. All digital data are updated at one sample/sec. The cross-plotted loads are displayed along with their strength envelopes at a computed update rate of 5 to 10 samples/sec. Hardcopies of the display are available in near-real time. These real-time dynamic displays allowed for the efficient and safe structural loads envelope clearance for the X-29A.

5.2 Structural Dynamics

Tracking of the aircraft structural dynamics was a key factor in the safe expansion of the flight envelope of the X-29A. Flight monitoring of the aircraft structural modal stability included both the airframe elastic modes, or aeroelasticity, and the FCS-elastic mode interaction, or aeroservoelasticity. Some twelve structural dynamic modes could be identified on the X-29A, of which the five most critical were tracked in real time in flight for all three flight control system modes (normal digital, ND; digital reversion, DR; analog reversion, AR). The five modes tracked in real time included the first symmetric and antisymmetric wing bending modes, the first fuselage vertical and lateral bending modes, and the first vertical fin bending mode. Flight-derived modal frequency and damping were compared in real time against closed-loop aeroservoelastic predictions and provided stability trend data as a function of airspeed as the flight envelope

was expanded. Of particular concern was monitoring for the onset of a potential dynamic interaction known as body-freedom flutter, or BFF. This was predicted to occur when the wing-first-bending-mode frequency decreased and coupled with the aircraft longitudinal short-period mode. Body-freedom flutter was predicted to act as a precursor to the static wing divergence. To date no BFF tendencies have been observed in flight. Flight data from the other seven structural modes were reduced and analyzed using postflight techniques.

Natural turbulence, pilot stick raps, and a wing flaperon eccentric rotary-mass excitation system were used to excite the aircraft structural modes. The flaperon rotary-mass excitation system used a frequency-sweep vibration input in an attempt to identify a predicted supersonic midflaperon torsion flutter mode. Typically the aircraft was stabilized in level flight for 1 to 2 min to perform the stick raps, the rotary-mass frequency sweeps, and for natural turbulence excitation.

The real-time data reduction technique consisted of a fast Fourier analysis method carried out on a Fourier analyzer using a flight data frame size of 1024 data samples at 100 samples/sec. The inverse Fourier transform was computed to obtain the autocorrelation function from which a data cutoff time could be manually selected. Smoothing the autocorrelation function yielded an autopower-spectrum display as a function of frequency (fig. 6) that was curve-fitted for each structural mode. The structural modal frequency occured at the maximum amplitude of the power spectrum density curve, and the structural damping was extracted using the half-power technique. More discussion of this technique can be found in reference 5. The flight-derived frequency and damping of the five primary structural modes were compared in real time with precomputed predictions as a function of aircraft equivalent airspeed (fig. 7).

Usually all three flight control modes were plotted and tracked at the same flight condition on the same data plot display to observe any aeroservoelastic effect. Adverse trends in frequency or damping of a particular structural mode would halt the flight envelope expansion until the phenomenon could be understood or further analyzed using postflight techniques.

5.3 Flight Control Systems

The safe and efficient flight testing of the X-29A required close monitoring of the dynamic stability levels because of the high degree of static instability and the minimal predicted stability margins at some flight conditions. A postflight data analysis method was used during initial envelope expansion flights for flight control systems clearance and dynamic stability checks. This process nominally required 1 to 3 days and allowed only one envelope expansion point be flown per flight to enable careful extrapolation of critical dynamic stability levels.

Efforts to improve flight productivity and safety resulted in the development of two new real-time dynamic stability techniques—one based on frequency response and the other based on time response. These methods improved flight test efficiency significantly by allowing multiple envelope expansion points on a single flight. The direct in-flight measurement of actual aircraft dynamic stability levels and online comparisons with preflight predictions also provided for enhanced safety.

Even though the X-29A longitudinal control system used multiple sensor feedbacks and a three-surface control effector mechanization (ref. 6), the control law did collapse into a single-loop configuration internally in the software. This allowed a classical open-loop frequency response technique to be used to assess longitudinal dynamic stability levels while maintaining all feedback loop closures. Pilot-generated frequency sweeps were used for excitation, and internal control system parameters were used for frequency response computations.

A diagram of the implemented technique is shown in figure 8. The internal control system parameters were telemetered to a ground computer, computations were performed using a fast Fourier transform algorithm, and the flight-determined frequency response was compared with a precomputed estimate based on simulation models. This technique provided a real-time comparison of predicted gain and phase margins with actual flight-determined values. This information was used to assess whether to proceed to the next flight test point immediately or to hold for further analysis.

A typical real-time graphical display is shown in figure 9. In general, the comparisons proved to be remarkably close, indicating that the mathematical models of the aircraft used in the predictive analyses were quite accurate. At one flight condition, the comparison was not too close, and a modification of the overall pitch loop gain was required to establish adequate stability margins. The successful modification (fig. 10) was made based solely on the frequency response results, attesting to the high quality data achievable using this technique.

A technique allowing real-time time response comparisons between flight and linear simulation data was also developed (ref. 7) to aid assessments of X-29A's flight control system performance. A technique similar to the one used for the frequency response tests was implemented. As shown in figure 11, aircraft sensor data was downlinked for use in ground computer algorithms, and computed results were displayed on graphical terminals. In the longitudinal case, pilot input signals were used as the input commands to a linear simulation of the aircraft. In the lateral-directional case, the aircraft's suface positions were used as a direct input into the simulation model equations. The output of the simulation was overplotted directly with the actual measured aircraft response parameters, thus allowing a real-time assessment of control system performance.

A typical comparison plot for a series of pulse maneuvers is shown in figure 12(a) for the pitch axis parameters and figure 12(b) for the lateral-directional axes parameters. The comparisons generally agreed closely and were sufficient to insure the aircraft motions were near those predicted and additional test points could be taken. Comparisons with linear simulation data rather than the full nonlinear simulation also allowed for easy detection of unexpected nonlinearities.

5.4 Aeroperformance

The X-29A aeroperformance real-time analysis technique development did not have a direct role in flight safety or flight envelope clearance. It was developed, rather, to increase flight efficiency and productivity through maneuver technique evaluation and data quality control to insure the best aeroperformance data possible. Direct real-time evaluation of the final data analysis product, as in the case of drag polar coefficients of lift and drag, minimized the number of flight repeats that often arise when postflight data reduction reveals poor data quality or poor flight maneuver technique such as unacceptably high maneuver dynamics. In addition to the value of immediate in-flight aircraft performance evaluation and immediate hard copy of flight results for postflight evaluation, the technique has the potential added bonus of utilization for real-time in-flight aerodynamic optimization of the aircraft.

The real-time aeroperformance data analysis method is based on the in-flight calculation of net thrust from static pressure measurements in the engine afterburner section. This algorithm was specially developed for the X-29A program by the Computing Devices Company (ComDev) of Ottawa, Canada and is known as the simplified net thrust method (SNTM). It is based on a complete thrust calibration over the power range of the flight test engine at the NASA Lewis Research Center Propulsion System Laboratory PSL-4 facility (ref. 8). The method is derived from the simplified gross thrust method (SGTM) developed 15 years earlier (ref. 9). The extension of the SGTM method to the SNTM method involved the real-time calculation of ram drag from true airspeed V_t and inlet mass flow rate. Net thrust was also corrected for estimated nozzle and spillage drag, yielding the net propulsive force F_{np}. A nominal accuracy of ± 3 percent was achieved from this algorithm for real-time net thrust calculation. Rapid engine throttle transients, performed to check the net thrust algorithm dynamic response, showed the algorithm could closely follow engine transient responses. Details of the method are found in reference 10.

Aircraft coefficients of lift C_L and drag C_D were calculated from the equations

$$C_D = \frac{D}{\bar{q}S} = \frac{F_{np} - F_{ex}}{\bar{q}S} \tag{2}$$

where excess thrust is computed from

$$F_{ex} = n_x W_t \tag{3}$$

and

$$C_L = \frac{L}{\bar{q}S} = \frac{n_z W_t - F_g \sin \alpha}{\bar{q}S} \tag{4}$$

Aircraft specific excess power P_s is also computed and displayed as a function of Mach number from the equation

$$P_s = F_{ex} V_t / W_t \tag{5}$$

The maneuver techniques used were the dynamic pushover-pullup and the constant-thrust, constant-Mach windup turn to sweep out a wide range of angle of attack at a given Mach number in two short maneuvers. These maneuvers were flown back-to-back at a nominal 0.20 *g*/sec *g*-onset rate at fixed Mach number increments over the speed range of 0.40 to 1.30 Mach. The maneuver pair could be completed in less than a minute. The real-time data inputs were neither filtered nor thinned. Data were plotted on the color graphics display at up to 12.5 times/sec, while columnar engine and aircraft digital data were updated once per second on the same display screen.

Figures 13 and 14 show representative displays of the quality of drag polars achieved. These real-time results were compared with later postflight-reduced drag polar results and were found to be in good agreement. Because of the decision not to digitally filter the aircraft accelerometers in real time, aerodynamic buffet onset could also be seen as a function of angle of attack and coefficient of lift on the drag polar and lift curves.

6. CONCLUDING REMARKS

Consideration for flight safety and efficient flight envelope expansion of the X-29A led to the development of several new, innovative, real-time analysis and display techniques. Critical X-29A technologies requiring the continuous in-flight monitoring included the forward-swept wing with its inherent tendency toward structural wing divergence and the large degree of airframe subsonic static instability. The real-time analysis techniques developed included structural static loads, structural dynamics, flight control system stability characteristics and aircraft flight response, and aeroperformance. Several of these analysis techniques also provided direct comparisons of flight-measured results with analytical predictions. These techniques greatly improved flight productivity both during the flight envelope expansion phase and the subsequent flight research phase, reducing the need for repeat flights or unnecessary postflight data reduction. The NASA Western Aeronautical Test Range capabilities enabled telemetry acquisition, real-time data processing, and display of the flight data in the mission control center.

REFERENCES

1. Sefic, W.J., and W. Cutler, "X-29A Advanced Technology Demonstrator Program Overview," AIAA 86-9727, April 1986.
2. Moore, Archie L., *The Western Aeronautical Test Range of NASA Ames Research Center*, NASA TM-85924, 1985.
3. Moore, Archie L., and Constance D. Harney, *Development of an Integrated Set of Research Facilities for the Support of Research Flight Test*, NASA TM-100427, 1988.
4. Hicks, John W., James M. Cooper, Jr., and Walter J. Sefic, *Flight Test Techniques for the X-29A Aircraft*, NASA TM-88289, 1987.

5. Kehoe, Michael W., *AFTI/F-16 Aeroservoelastic and Flutter Flight Test Program — Phase I*, NASA TM-86027, 1985.

6. Gera, Joseph, and John T. Bosworth, *Dynamic Stability and Handling Qualities Tests on a Highly Augmented, Statically Unstable Airplane*, NASA TM-88297, 1987.

7. Bauer, J.E., D.B. Crawford, D. Andrisani, and J. Gera, "Real-Time Comparison of X-29A Flight Data and Simulation Data," AIAA 87-0344, Jan. 1987.

8. Burns, Maureen E., and Thomas A. Kirchgessner, *Airflow Calibration and Exhaust Pressure Temperature Survey of an F-404, S/N 215-209, Turbofan Engine*, NASA TM-100159, 1987.

9. Kurtenbach, Frank J., Evaluation of a Simplified Gross Thrust Calculation Technique Using Two Prototype F100 Turbofan Engines in an Altitude Facility, NASA TP-1482, 1979.

10. Ray, R.J., J.W. Hicks, and R.I. Alexander, *Development of a Real-Time Aeroperformance Analysis Technique for the X-29A Advanced Technology Demonstrator*, NASA TM-100432, 1988.

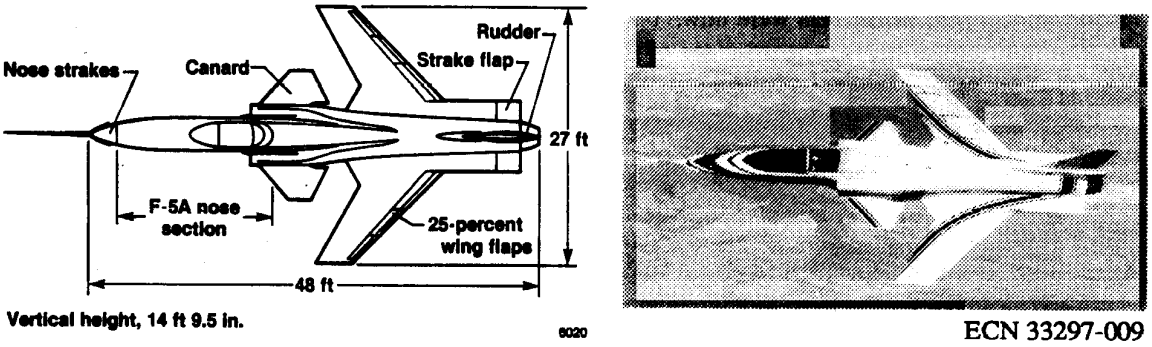

Figure 1. X-29A advanced technology demonstrator.

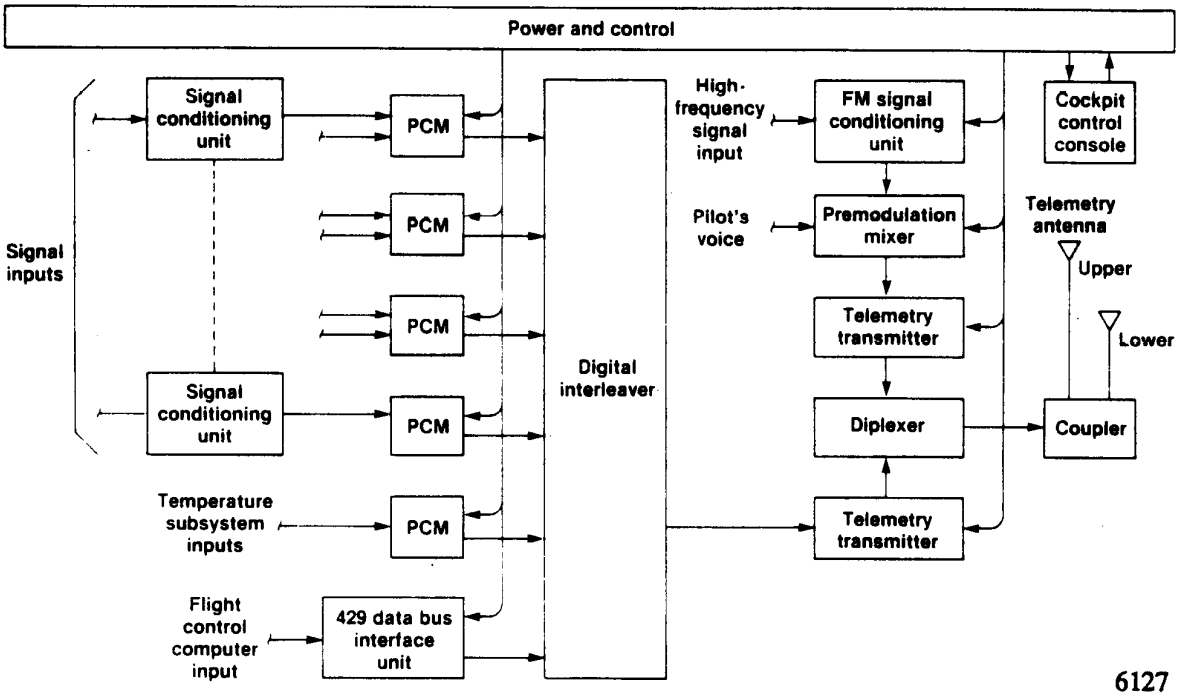

Figure 2. X-29A on-board data acquisition system.

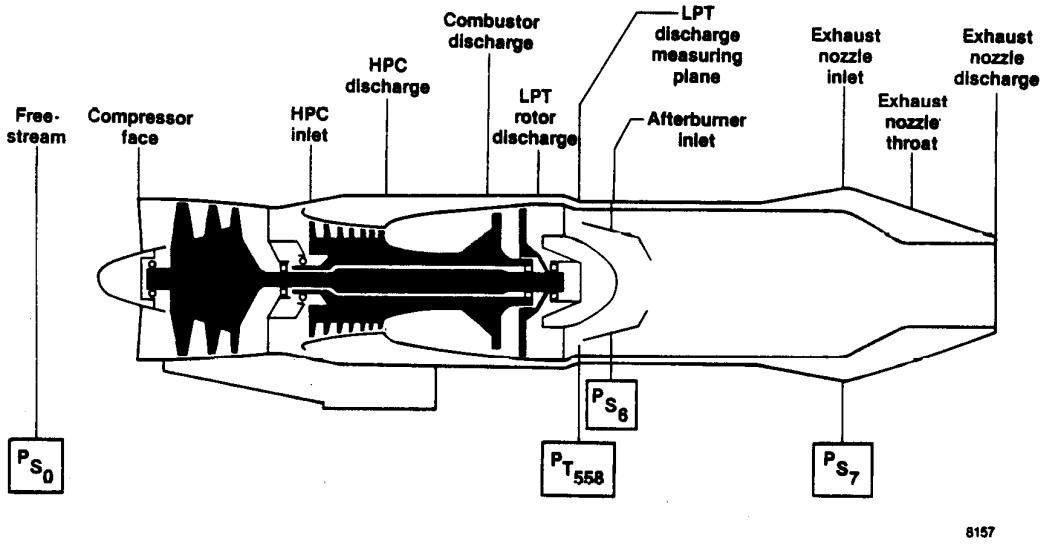

Figure 3. Engine instrumentation system.

EC 88-0019-001

Figure 4. Western Aeronautical Test Range mission control center.

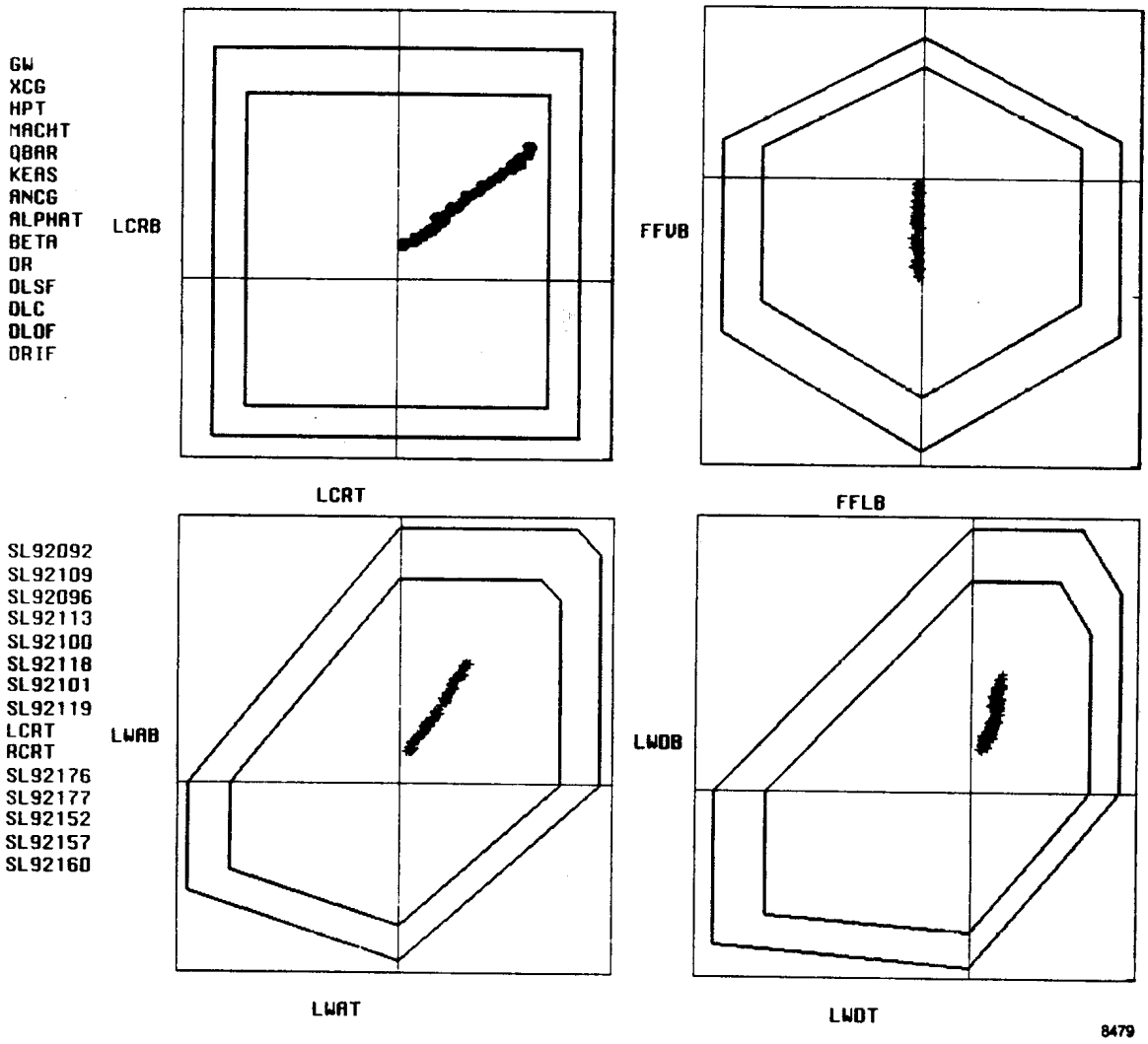

Figure 5. Hard copy version of real-time aircraft structural loads graphics display.

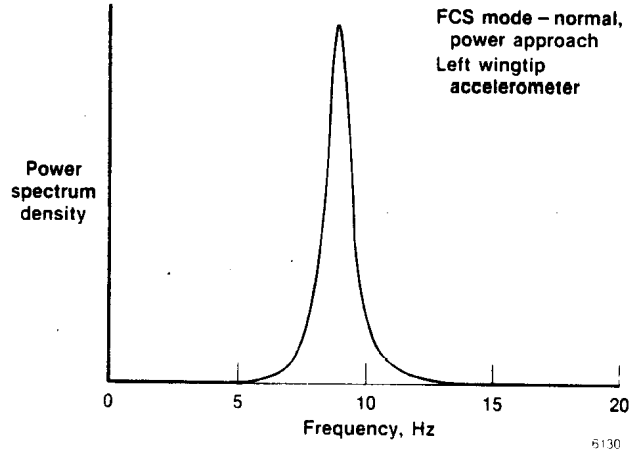

Figure 6. Parabolic curve fit to determine structural frequency and damping in real time.

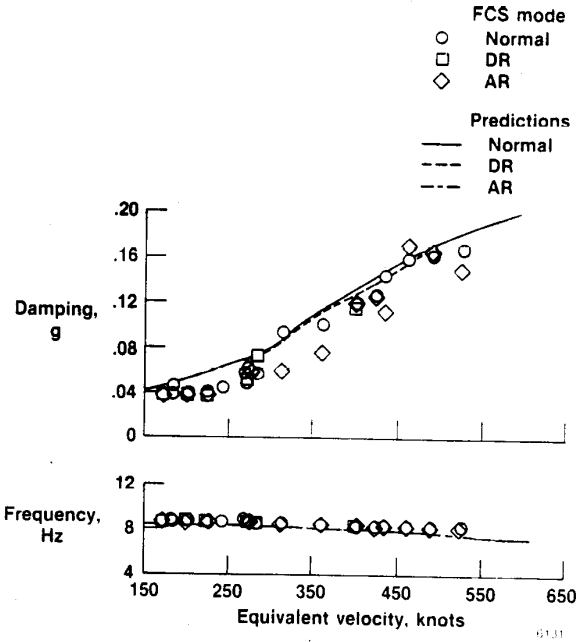

Figure 7. Structural mode frequency and damping characteristics.

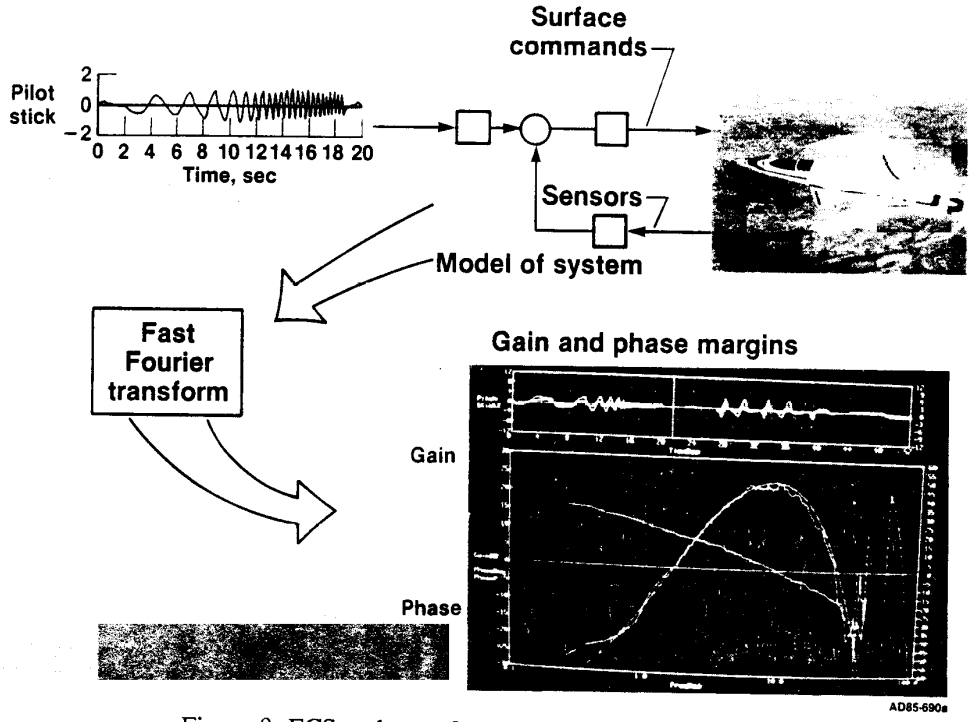

Figure 8. FCS real-time frequency response flow chart.

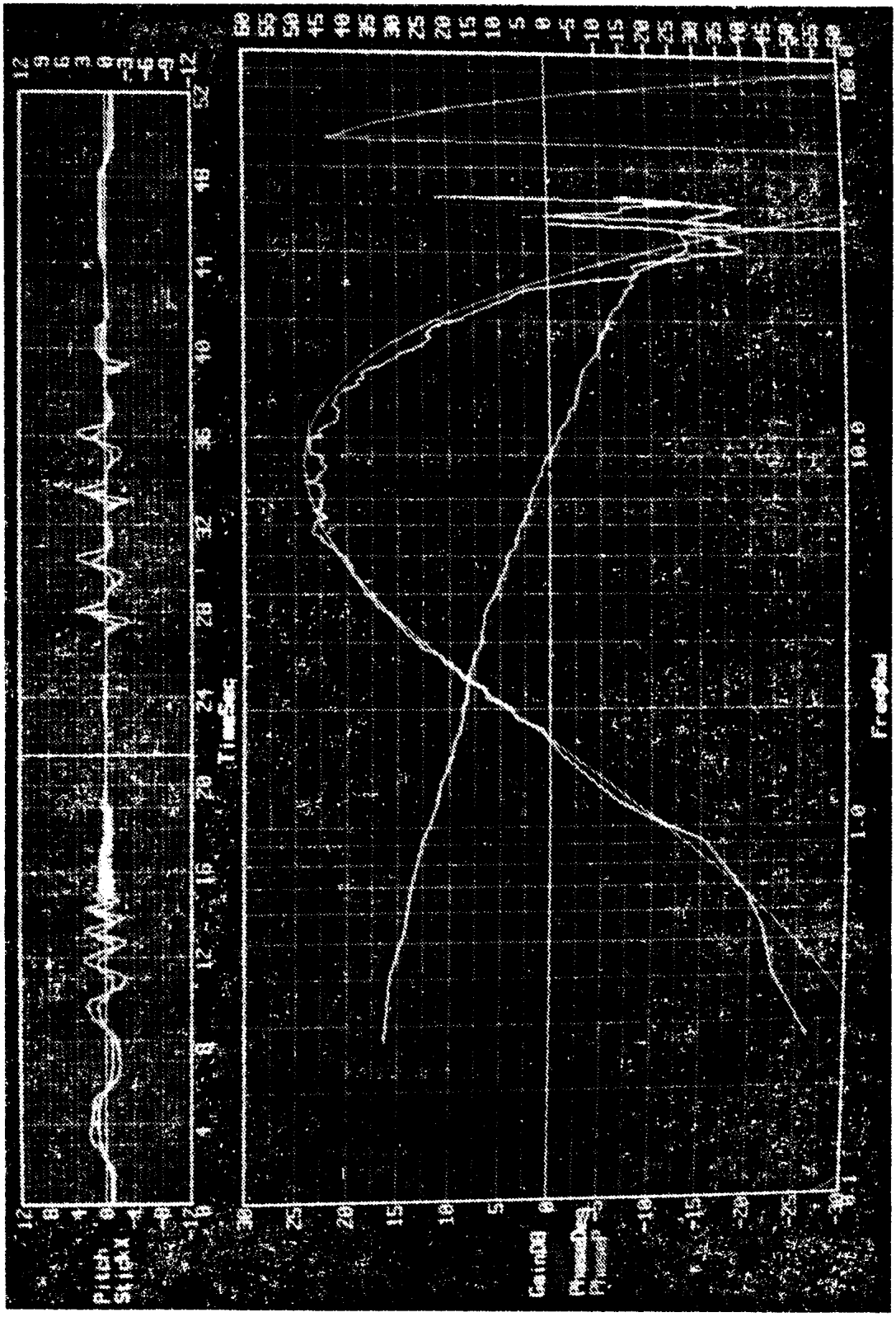

EC 86-33511-001

Figure 9. Photo of real-time FCS frequency response graphics display.

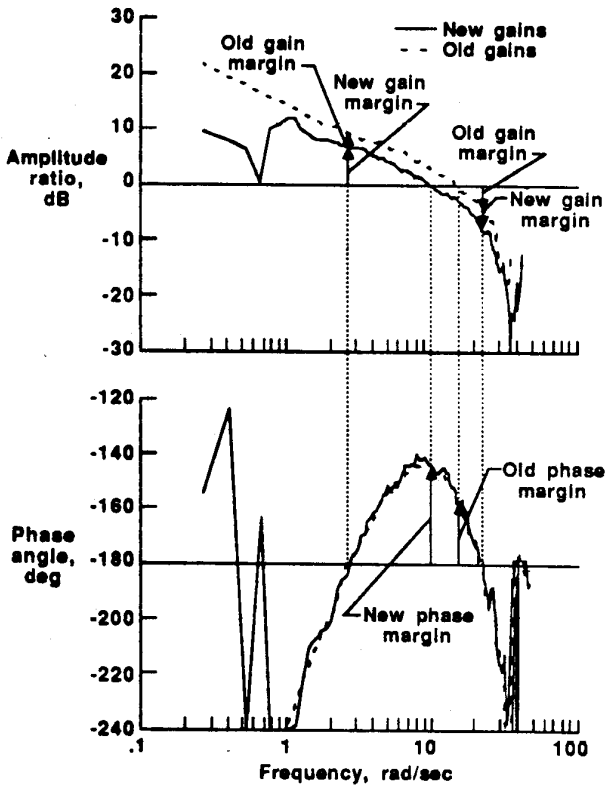

Figure 10. Effect of gain change on flight-measured Bode plot.

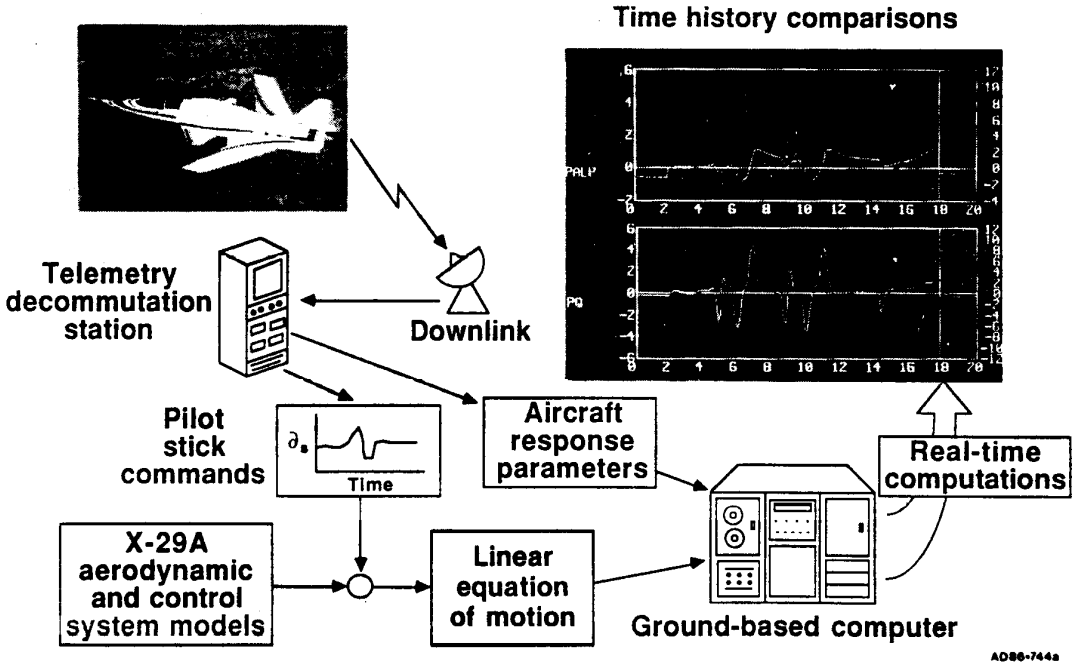

Figure 11. Aircraft flight response characteristics flow chart.

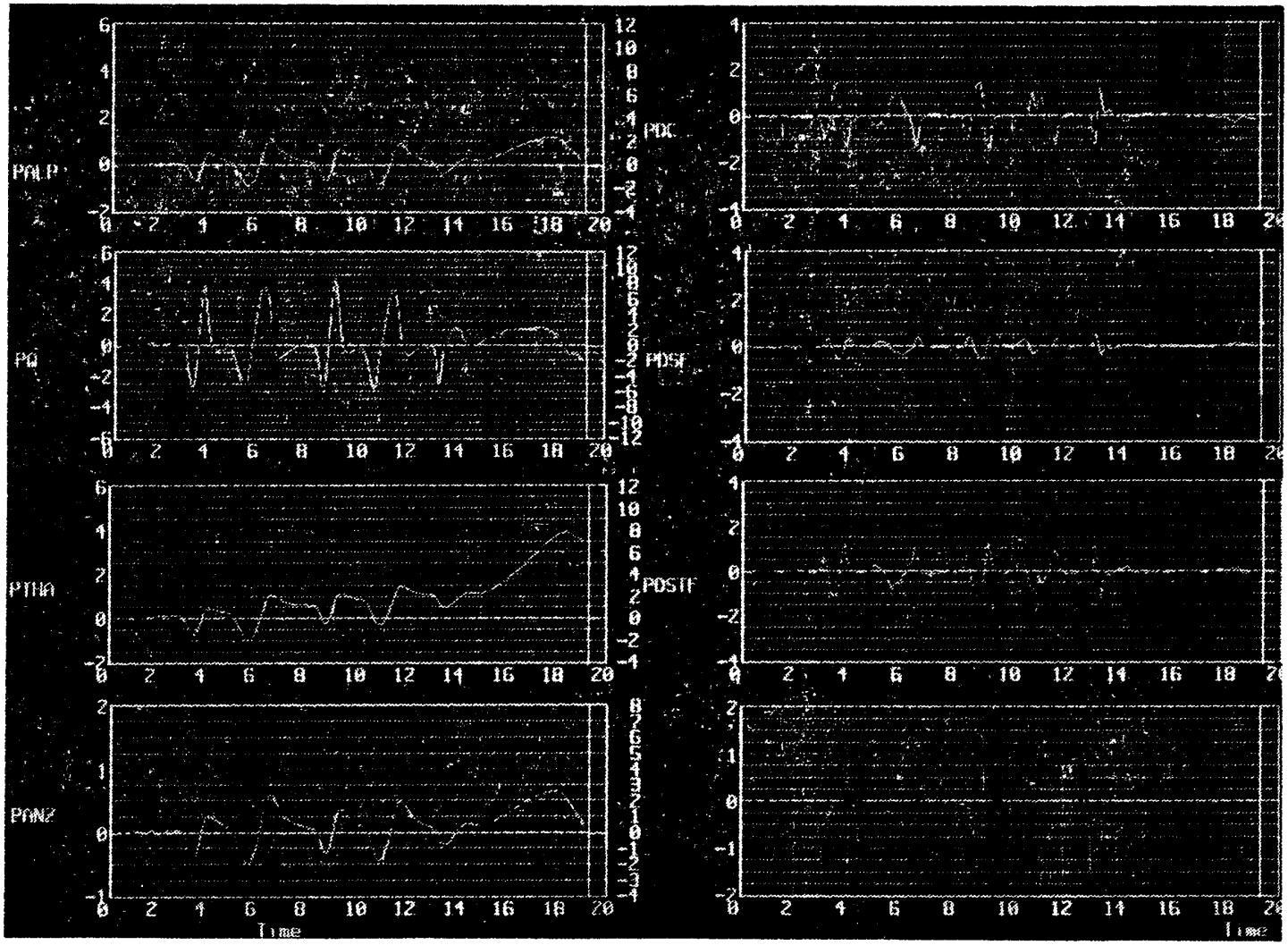

EC 88-0173-001

(a) Longitudinal.

Figure 12. Photos of graphics displays of time history comparison of real-time linear simulation data and flight data.

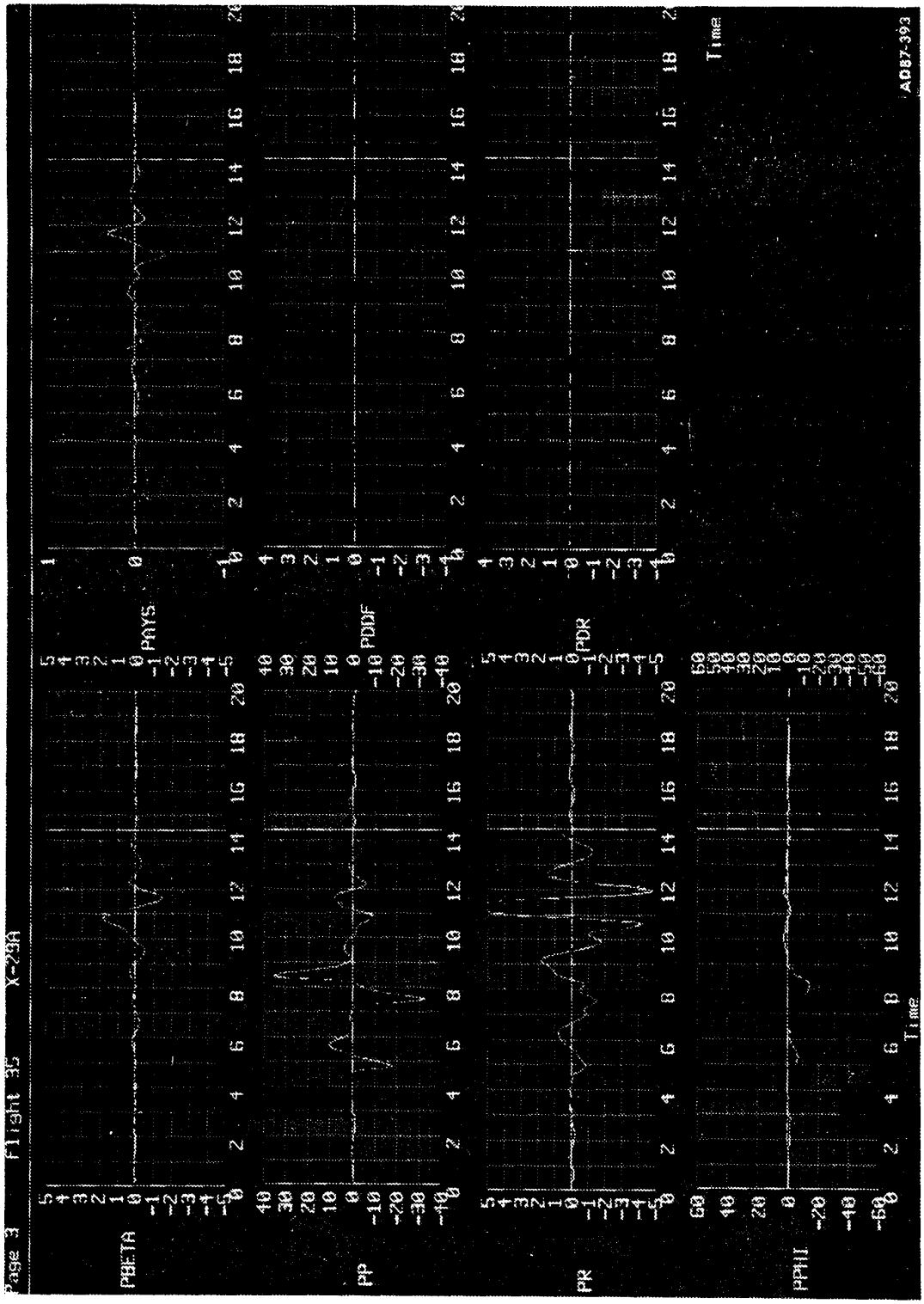

(b) Lateral-directional.

Figure 12. Concluded.

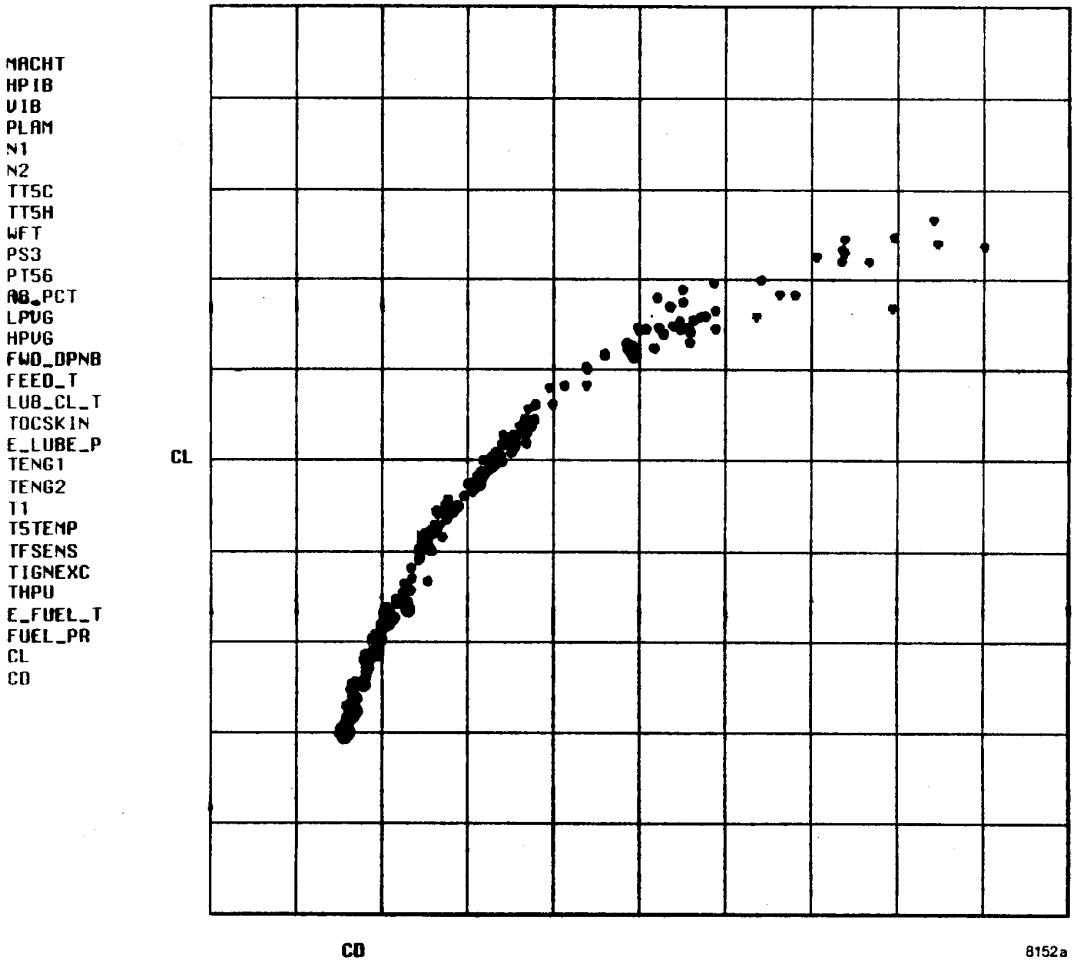

Figure 13. Hard copy version of real-time windup turn-generated drag polar.

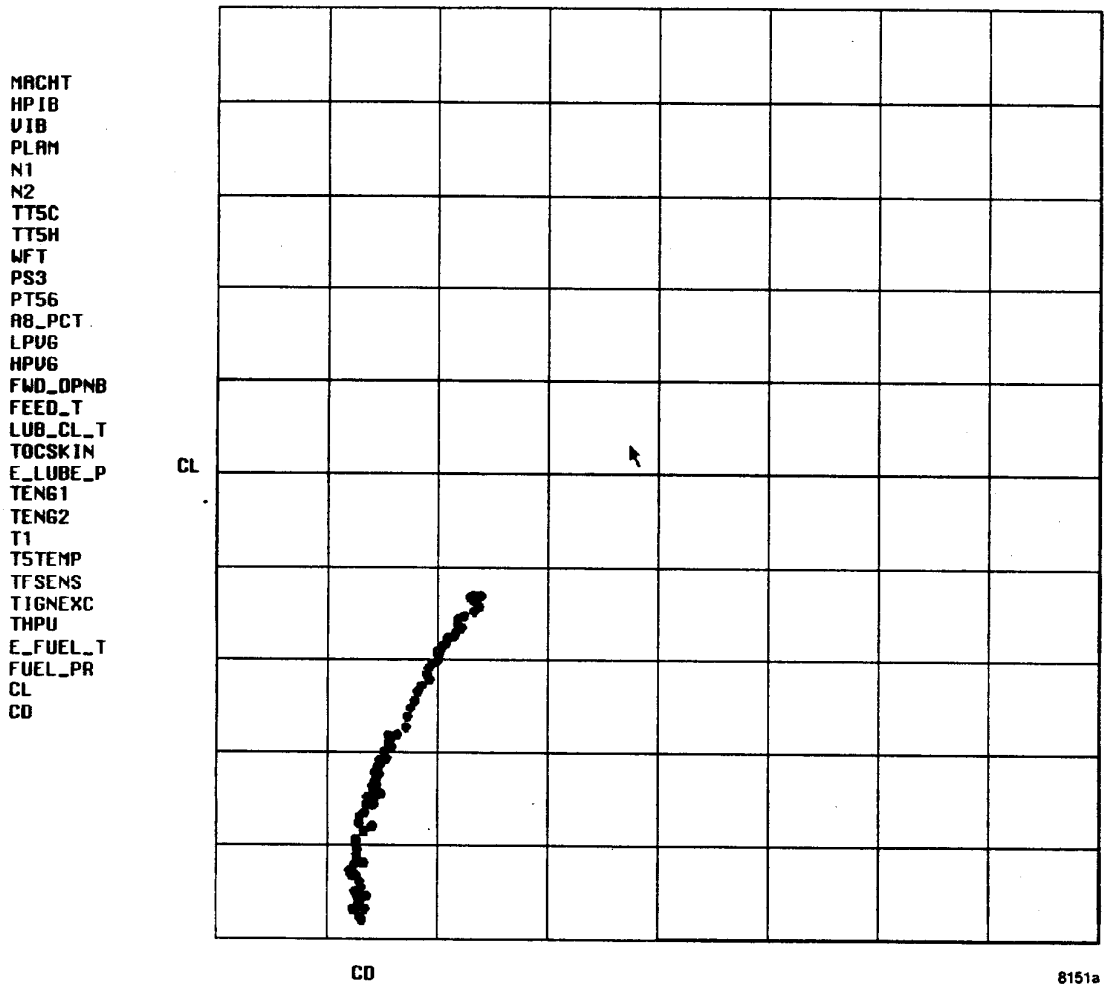

Figure 14. Hard copy version of real-time pushover-pullup-generated drag polar.

NASA
National Aeronautics and Space Administration

Report Documentation Page

1. Report No.	2. Government Accession No.	3. Recipient's Catalog No.
NASA TM-101692		

4. Title and Subtitle

Real-Time Flight Test Analysis and Display Techniques for the X-29A Aircraft

5. Report Date
November 1988

6. Performing Organization Code

7. Author(s)
John W. Hicks and Kevin L. Petersen

8. Performing Organization Report No.
H-1520

10. Work Unit No.
RTOP 533-02-51

9. Performing Organization Name and Address
NASA Ames Research Center
Dryden Flight Research Facility
P.O. Box 273, Edwards, CA 93523-5000

11. Contract or Grant No.

13. Type of Report and Period Covered
Technical Memorandum

12. Sponsoring Agency Name and Address
National Aeronautics and Space Administration
Washington, DC 20546

14. Sponsoring Agency Code

15. Supplementary Notes

Prepared for presentation as Paper No. 6 at AGARD 73rd Flight Test Techniques Symposium Flight Mechanics Panel, Edwards Air Force Base, California, October 17–20, 1988.

16. Abstract

The X-29A advanced technology demonstrator flight envelope expansion program and the subsequent flight research phase gave impetus to the development of several innovative real-time analysis and display techniques. These new techniques produced significant improvements in flight test productivity, flight research capabilities, and flight safety.

These techniques include real-time measurement and display of in-flight structural loads, dynamic structural mode frequency and damping, flight control system dynamic stability and control response, aeroperformance drag polars, and aircraft specific excess power. Several of these analysis techniques also provided for direct comparisons of flight-measured results with analytical predictions. The aeroperformance technique was made possible by the concurrent development of a new simplified in-flight net thrust computation method. To achieve these levels of on-line flight test analysis, integration of ground and airborne systems was required. The capability of NASA Ames Research Center, Dryden Flight Research Facility's Western Aeronautical Test Range was a key factor to enable implementation of these methods.

17. Key Words (Suggested by Author(s))	18. Distribution Statement
Flight test Forward-swept wing Real-time analysis X-29A	Unclassified — Unlimited Subject category 05

19. Security Classif. (of this report)	20. Security Classif. (of this page)	21. No. of pages	22. Price
Unclassified	Unclassified	20	A02